Fifteenth USA/Europe Air Traffic Management Research and Development Seminar (ATM2023)

Multiple Aircraft in a multi-criteria Trajectory Optimization

Judith Rosenow, Thomas Zeh, Martin Lindner,
Stanley Förster and Hartmut Fricke
Institute of Logistics and Aviation
Technische Universität Dresden
Dresden, Germany
Judith.Rosenow@tu-dresden.de

Alexis Caraud
Laboratory of Applied Mathematics
Ecole Nationale de l'Aviation Civile (ENAC)
Toulouse, France
Alexis@Caraud.fr

***Abstract*—In recent years, the optimization of the trajectory has developed into a philosophical problem with arbitrary objective functions and assumptions made by conflicting stakeholders. What has remained since 1987 is that trajectories that have been locally optimized in advance must share an airspace that is severely limited by the local optima without getting into conflicts. This problem is now being solved on various numerical scales by various entities with differently weighted foci on either the (local) trajectory side or the (global) interaction side. Most of the approaches make some serious compromises on the non-focused side. The simulation-based environment for single aircraft trajectory optimization, TOMATO, has been developed for high accuracy of optimized single trajectories and has now been expanded for aircraft separation concerns. In this study, TOMATO is used to construct a set of single optimum conflict-free trajectories. By identifying overloaded airspaces, determining main tracks in overloaded airspace, and providing track- and flight level-specific airspace costs, we could reduce the number of overloaded airspaces from 9 to 2 and the total number of potential conflicts from 336 to 198 without a significant increase in fuel burn or flight time. The approach could be used in decision support tools for a network manager by providing feedback for flight planning and air traffic service entities.**

***Keywords*—Aircraft Trajectory Optimization, Air Traffic flow management, Air Traffic Management, Air Traffic Control**

I. Introduction

Six degrees of freedom and the sometimes conflicting interests of at least three different stakeholders complicate the optimization of aircraft trajectories in four-dimensional space. The task becomes even more complex the more aircraft are simultaneously in the airspace and have to be safely operated. This task, which has been summarized by Odoni [1] under the term Air Traffic Flow Management (ATFM), is currently solved on different numerical scales by different entities with the help of human intuition and a variety of decision support tools. An automated solution approach has been the subject of research for 45 years.

In general, Air Traffic Management (ATM) is the provision of facilities, procedures, and seamless services in collaboration with all parties involving airborne and ground-based functions. According to the International Civil Aviation Organization (ICAO), ATM is the dynamic, integrated management of air traffic and airspace and includes Air Traffic System (ATS), Air Space Management (ASM), and ATFM [2].

However, an increasing cost pressure, as well as growing political and public awareness of the climate impact of air transport, increase the attractiveness of a global, multi-criteria optimized air transport system that takes into account all stakeholder interests, that does without a fixed waypoint structure and enables a Free Route Airspace (FRA). The current procedure-driven approach does not fit the requirements of an optimization task in such a complex environment. Therefore, reliable automated decision support for all three subsystems ATS, ASM, and ATFM is needed.

One of the biggest challenges of ATM is the range of the scales, as a large number of individually optimized trajectories must operate simultaneously without loss of separation in limited airspace. On the one hand, aircraft operators and ATS strive for optimum single aircraft trajectories. On the other hand, ATFM aims to prevent local demand-capacity imbalances by adjusting the flows of aircraft. There are numerous hybrid approaches between trajectory optimization and ATFM. Depending on the application, the focus of optimization is more on one side or the other. The more aircraft type-specific criteria are taken into account (i.e. the stronger the focus is on trajectory optimization), the less attention is put on potential conflict among multiple aircraft. This results in realistically optimized trajectories, but with very limited consideration of the ATFM constraints. On the other hand, ATFM-heavy solution proposals are often based on unrealistic individual trajectories. The simulation-based environment for single aircraft trajectory optimization TOolchain for Multi-criteria Aircraft Trajectory Optimization (TOMATO) [3] has been extended with ATFM-related problems in the past years while maintaining the high accuracy of the optimized single trajectories. Today, TOMATO can only evaluate hybrid ATFM scenarios. In this study, a set of single optimized conflict-free trajectories are calculated with TOMATO by avoiding the congestion of individual airspaces and leveling the complexity

This work is financed by Deutsche Forschungsgemeinschaft (DFG, German Research Foundation) in the framework of the project UBIQUITOUS-410540389F.

of the airspace.

A. State of the art

Usually, approaches of ATFM optimization are solved either with machine learning or are simplified to linear optimization problems. Machine learning approaches focus on capacity prediction and minimizing overloaded airspaces by iteratively adjusting all trajectories within a predefined range [4]. Salaun et al. [5] processed those capacity forecasts for designing traffic flow management strategies and optimizing capacity allocation, based on a fixed waypoint structure without considering the efficiency of single trajectories. On the other hand, Gariel et al. [6] used clustering techniques to learn nominal spatial trajectory patterns for terminal airspace monitoring for separating trajectories in the Terminal Manoeuvring Area (TMA) and Sabhnani et al. [7] optimized en-route sectors with well-structured air traffic patterns after clustering the trajectories in the cruise phase. However, all these data-driven approaches analyze real trajectories with unknown fuel efficiency and do not focus on single-trajectory optimization targets.

On the other hand, Bertsimas, Odoni, et al. [8] formulated an Integer Program (IP) for reducing capacity overloads at specific altitudes without allowing altitude changes. The idea has been extended and improved by many authors, e.g. Balakrishnan and Chandran [9] developed an IP for producing lateral options when faced with capacity restrictions that are unpredictable and therefore represented by probabilistic scenario trees. Again, those optimization strategies do not consider the single trajectories optimality.

Toratani et al. [10] formulated the trajectory optimization as an Optimal Control (OC) problem and subsequently the sequence optimization as a Mixed-Integer Linear Programming (MILP) problem. Thereby the results of the trajectory optimization were reduced to the arrival time of each aircraft and the Required Time of Arrival (RTA) was used as a decision variable for connecting both optimizations. An interesting mixed-integer formulation has been applied to an OC-based trajectory optimization, where Soler et al. discretized the problem into a Mixed-Integer Nonlinear Programming (MINLP) problem [11]. These approaches promise near-exact solutions for optimal sequencing and separation of optimized aircraft trajectories at a single point. However, the complexity of the method does not allow ATFM optimization with a high number of "merging points". Furthermore, those methods do not rely on multi-criteria-optimized aircraft trajectories.

One proposed solution is to focus more on optimal trajectories and take an iterative approach to minimize potential conflicts by considering traffic flows per airspace. The simulation environment TOMATO is a toolchain for flexible trajectory optimization. So far, with TOMATO the number of potential conflicts and task load has been calculated and considered as a cost layer in the pathfinding module. However, this procedure distributes air traffic patterns more homogeneously with diversions around overloaded airspaces. The procedure does not necessarily lead to a reduced number of potential conflicts but to an increase in fuel burn [12]. In this study, we propose our new method with track-specific airspace costs to homogenize the traffic flow. These track-specific airspace costs are charged either to all aircraft or to randomly chosen aircraft in overloaded airspaces.

II. Simulation environment TOMATO

The iterative simulation-based optimization tool TOMATO is used to optimize aircraft trajectories. TOMATO is made up of three control loops that are iteratively coupled to one another (see Figure 1). TOMATO models and accesses predefined (e.g. real) individual trajectories, whereby missing input variables (e.g. typical masses, speeds, climb and descent rates, optimum altitudes) are calculated. Individual trajectories are optimized depending on the type of input variables. Air traffic scenarios are simulated, assessed, and optimized regarding different optimization functions. In this paper, we focus on the hybrid optimization of a conflicting air traffic scenario considering individually optimized trajectories. Depending on the optimization target function and on the type of input variables, a path-finding module based on the A* algorithm [13] interacts with the flight performance model Sophisticated Aircraft Performance Model (SOPHIA) [14]. Considering the semicircular rules (odd flight levels for tracks between $0°$ and $179°$) the path-finding algorithm provides optimized lateral paths for all possible flight levels. Specifically, between $\mathrm{FL}_{\min}$ = 250 and $\mathrm{FL}_{\max}$ = 400, eight iterations are in each blue loop in Figure 1. After SOPHIA has calculated the vertical profiles along all paths, the cheapest (regarding fuel costs or time costs) is stored. This coupling between lateral and vertical aircraft trajectory optimization with a high degree of aircraft performance precision is a special feature of TOMATO. This inner control loop (see blue lines in Figure 1) will be neglected if the flight level is predefined, or if a flight utilizes an individual performance-optimized continuous cruise climb procedure [15]. However, the latter method is not necessarily weather-optimized as vertical avoidance of unfavorable winds is excluded. For the future, the implementation of a bisectional search is planned for optimizing step climbs. In the case of a target function, in which corresponding air speed is neither analytically calculable nor predefined, for each flight, weighting functions (e.g. contrail costs should constitute not more than $30\,\%$ of the total costs) can be defined. After SOPHIA has calculated the vertical profiles along all paths, the resulting cost ratios are compared with the predefined weighting functions. Subsequently, the cost layers in the path-finding algorithm are adjusted (see gray lines in Figure 1). After all flights are individually optimized, the scenario is evaluated regarding conflicts and controller task load (depicted as purple lines in Figure 1). Using an arbitrary airspace structure, distances and times between all 4D trajectories are calculated, potential conflicts are derived, overloaded airspaces are identified, main traffic flows are extracted, and a new path-finding layer with airspace costs is defined, which then affects the next iteration. The procedure is described in Section III. Note, in order to make efficient use of the computing capacity, flight power-based vertical optimization is dispensed with when all three control loops are used. In this case, we do not use step climbs.

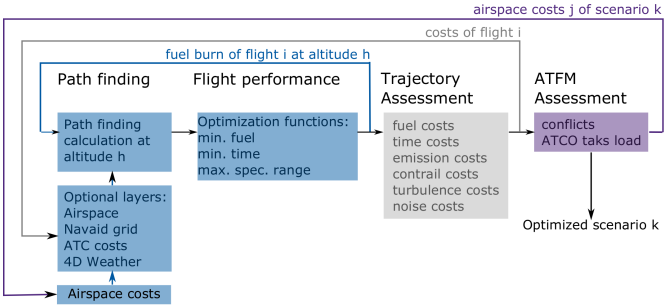

Figure 1: Three interlaced control loops of TOMATO for an optimized air traffic scenario.

A. *Trajectory Optimization with TOMATO*

The first step of our optimization procedure is the path-finding in the inner loop of Figure 1. It utilizes various grids to establish nodes and edges, including ATS routes [16], free optimization with either a graticule grid with the pole located at the departure [3] or a hexagonal grid [17] and a specialized grid for departing flights [18]. As graph-based algorithms like the A* cannot include either the flight performance modeling or time-based costs directly, those effects must be included in the costs of the edges. To this end, TOMATO adds, removes, and updates various cost layers during optimization, depending on the desired objectives. Besides typical cost layers, such as emission costs, the weather impact, and airspace layers such as overfly charges or restricted areas, some special features distinguish TOMATO from other aircraft trajectory optimization tools. For example, contrail costs, identified after the first trajectory assessment (gray loop), support a desired cost weighting [19]. Furthermore, airspace costs can be derived after the first ATFM assessment (purple line) to distribute flights iteratively for an optimized and homogeneous air traffic flow [20]. Especially for lower altitudes, aircraft noise constitutes a further optional layer. The single event levels L_{SEL} are calculated according to the European Civil Aviation Conference (ECAC) Doc. 29 [21, 22], which are then evaluated in the path-finding algorithm and the subsequent assessment [23].

These targets are usually combined with time-specific 3D weather data sets from the Global Forecast System (GFS) [24], which require the calculation of an approximated aircraft position for each corresponding weather data set in the path finding [3, 17, 25]. For this approximation, we generated aircraft-type and mass-specific tabulated aircraft performance data, which contain airspeed, rate of climb, thrust, and fuel flow depending on the phase of flight and altitude [18]. This tabulated aircraft performance allows estimating the particular aircraft's performance during path-finding so that 4D weather data can be obtained at the predicted position, altitude, and point in time. Additionally, these tables are also used to estimate the thrust in the noise layer during path finding [23]. The tabulated aircraft performance is another special feature of TOMATO, which enables the introduction of time-dependent costs like dynamic weather in the path finding of the A*.

As the tabulated aircraft performance serves only as an estimation during path-finding, the second step is the flight performance calculation with the kinetic model SOPHIA to create a high-precision vertical profile. SOPHIA calculates either a predefined or an optimum vertical profile along the provided/optimal lateral path with a set of different target functions [14]. Typical optimization target functions are minimum fuel, – time, – noise or – emissions, minimum total costs, environmental costs, direct operating costs, minimum conflicts, or minimum controller task load. SOPHIA uses analytical functions for calculating the state variables v_{TAS}, pressure altitude p [Pa], and flight path angle γ for each time step. For the optimal speeds of minimum fuel or maximum specific range, however, an analytic solution cannot be obtained, so Brent's method [26] is used to compute these particular speeds. In an aircraft type-specific proportional-integral-derivative controller (PID controller), $v_{\mathrm{TAS,target}}$, p_{target}, and γ_{target} are employed as controlled variables and the lift coefficient c_L is used as regulative variable [14]. Other targets, especially multi-criteria optimization targets are achieved iteratively within the trajectory assessment loop (gray).

The profile is described by the true airspeed v_{TAS} [m/s], thrust F [N], fuel flow $\dot{m}_f$ [kg/s], forces of acceleration a_x [m/s^2] and a_y [m/s^2] for the derivation of v_{TAS}, time of flight t [s], and emission quantities [kg/s] [27]. Each time step (default 1 s), the state variables are calculated in the ground-based coordinate system including wind correction. Rosenow et al. [14] describe the physical fundamentals of SOPHIA, including aerodynamic modeling. The flight performance can be modeled for different jet-engine powered aircraft types, which require type-specific parameters for the physical model. The Open Aircraft Performance model (OpenAP) [28] provides these parameters for the drag polar depending on the flap handle position, the engine thrust depending on the throttle parameter or defined ratings, and the resulting fuel flow. Furthermore, OpenAP contains relevant characteristics of the aircraft type, like the wing area S [m^2], the maximum Mach number M_{MO}, the maximum calibrated airspeed V_{MO}, the number of engines, and the aircraft mass limitations. For the quantification of the fuel burn and the engine emissions for environmental costs, the model is enriched with our jet engine combustion model [27].

The profile can be constructed out of an arbitrary number and combination of five distinct flight phases; take-off, climb, cruise, descent, and landing. Take-off, holding and landing are optional but have to be at once at the beginning or end, respectively, if used. Any number of the climb, cruise, and descent phases can be used, but the combinations must be conclusive regarding the order and end triggers. For profiles not starting with a take-off phase, initial conditions of the state variables v_{TAS}, H, and γ are required for the first phase, which can be fixed or free [29].

If several phases are combined, so-called end triggers initiate the transitions, which detect the end of a flight phase and continue with the next one in the list. These end triggers are defined with parameters (e.g. along-track distance Δs and flight duration Δt, altitude p_{target}, calibrated airspeeds v_{CAS}, and flight path angle γ for distinctive descent phases [30])

or events (lift-off, touch-down, passing of certain waypoints (WPT) or the Top of Descent (TOD)).

For the trust F, the ratings maximum take-off F_{MTO}, maximum climb F_{MCL} and idle F_I are available from OpenAP [28]. Additionally, SOPHIA computes the thrust required F_{req} to maintain current altitude and speed as well as the thrust required for a desired path angle $F_{req,\gamma}$ for non-idle descents. F_{MTO} and F_{MCL} can be reduced with the de-rating factor f_F. The lift L and drag D can be adjusted with the flap parameter δ_f [0...1], gear parameter δ_g [Boolean] (both OpenAP [28]) and speedbrake parameter δ_s [0...1] (specific for SOPHIA with an aircraft-type-specific parameterisation [30]).

Constant operating speeds can be specified as v_{TAS}, v_{CAS} or Mach number M, with the option for an automatic switch between v_{CAS} and M during climb or descent at the individual cross-over altitude [29]. Functions for optimal operating speeds depending on the flight phase and the desired target. During the climb, either γ or the rate of climb v_{ROC} can be maximized. The cruise phase can be optimized with the maximum specific range SR, while the descent maximizes the lift-to-drag ratio L/D. Table I summarizes the most important parameters and associates them with the typical flight phase.

B. Trajectory Assessment

The optimization assessment distinguishes among Direct Operating Costs (DOC), delay costs, and environmental costs. To the latter, we assign contrail costs depending on the time of the day and year and latitude [19]. Among the DOC, staff ($1{,}6\,\mathrm{e}$ per minute per flight crew member, $0{,}7\,\mathrm{e}$ per minute and cabin crew member [31]), insurance and maintenance [31, 32] costs depend on flight time. Fuel costs (accounting for $25\,\%$ to $30\,\%$ of DOC) are frequently adapted according to the International Air Transport Association (IATA) fuel price monitor [33]. Costs for air traffic control, charges of en-route, and terminal navigation services are factored worldwide according to the principles of the particular Air Navigation Service Provider (ANSP). Airport handling and dispatching fees, representing a $15\,\%$ share of DOC, as well as indirect operating costs, don't have an influence on trajectory optimization, so they are not considered. Delay costs are estimated based on Cook [31], enhanced by passenger-specific compensation costs including costs for flight canceling and re-booking [34]. Aircraft engine emissions (approximately $3160\,\mathrm{g}$ carbon dioxide CO_2, $1240\,\mathrm{g}$ water vapor H_2O, $14\,\mathrm{g}$ nitric oxides NO_x, $0{,}025\,\mathrm{g}$ soot [35]) are transferred into costs by using emission- and location-specific values of Global Warming Potential (GWP) [35] for estimating carbon dioxide equivalent (CO_2-eq.) emissions. Contrail induced CO_2-eq. emissions are assessed according to [19, 36] CO_2-eq. emissions are converted into costs using the Emission Trading System (ETS), whereby the costs per EU Allowance (EUA) are frequently adapted according to [37].

C. ATFM Assessment

In this paper, TOMATO was extended to include ATFM optimization. Therewith, for the first time, TOMATO can consider ATFM concerns. The goal is for individually optimized trajectories to be considerate of each other, orient themselves to each other and iteratively order themselves within overloaded airspaces. In addition, the aim is to achieve a cost minimum between flying through congested airspace with increased airspace costs in the path search algorithm and avoiding the preferred flight level with increased fuel consumption in the flight performance evaluation. This coupling is unique to the authors' knowledge. The method developed for this purpose is described in Section III

III. Iterative ATFM optimization

The idea of the developed procedure is derived from the mathematical description of the controller's task load. The controller's task load decreases with decreasing variation of aircraft tracks per flight level, as potential conflicts between crossing air traffic are more complex to be solved than conflicts within a directed flow. From this follows, a few uniform traffic flows, which do not necessarily have to follow a static airway structure, are desirable per airspace. An economically controlled preference for individual tracks per airspace would therefore reduce the controller's task load. A reduced controller's task load would allow more aircraft to cross the desired airspace.

From the assumptions mentioned above, we derived the following outer optimization loop (purple loop in Figure 1):

1) find overloaded airspaces (Subsection III-A)
2) identify main traffic flows within those airspaces (Subsection III-B)
3) calculate airspace-, altitude-, and track-specific costs for an airspace cost layer in the path-finding algorithm (Subsection III-C)
4) re-run the whole TOMATO process for those aircraft in conflict and convince intruding aircraft to either follow a main traffic flow or vertically and/or laterally avoid the overloaded airspace (Subsection IV)

The termination criterion of the optimization is the minimum total number of potential conflicts.

A. Identification of overloaded airspaces

Since the airspace structure (i.e. the sector size, shape, and position) is volatile, in this study and for the assessment, we divide the airspace in uniform graticule airspaces with a grid size of $\Delta\lambda = \Delta\phi = 1^\circ$ (see Figure 2 for the size of the uniform airspaces in relation to a single flight). In total, 90 airspaces are analyzed.

For each airspace, we calculate the number of potential conflicts and the task load. Potential conflicts are defined by less than 2000 feet of vertical separation and/or $5\,\mathrm{NM}$ of horizontal separation between two aircraft [2, 20].

As soon as the number of conflicts exceeds $N_{\max} = 10$, we define and store the airspace as overloaded airspace and cluster the tracks of all aircraft to identify some main traffic flows.

B. Identification of main air traffic flows

In order to find out which track already dominates in the overloaded airspace (so-called main traffic flows), the

TABLE I. Choices of parameters to specify each flight phase in TOMATO

Parameter	Take-off	Climb	Cruise	Descent	Holding	Landing
Altitude	—-	—-	const. p, opt. p	—-	const. p	—-
Speed	—-	$\max \gamma$, $\max v_{\mathrm{ROC}}$, v_{TAS}, v_{CAS}, M	$\max SR$, v_{TAS}, v_{CAS}, M	$\max L/D$, v_{TAS}, v_{CAS}, M	$\min \dot{m}_f$	—-
Thrust	$F_{MTO} \cdot f_F$	$F_{MCL} \cdot f_F$, $F_{MTO} \cdot f_F$	F_{req}	F_I, $F_{req,\gamma}$	F_{req}	—-
Configuration	δ_f	δ_f, δ_g, δ_s	δ_f, δ_g, δ_s	δ_f, δ_g, δ_s	—-	δ_f
End trigger	$L > W$	p_{target}, Δt, Δs	WPT, TOD, Δt, Δs	p_{target}, γ, Δt, Δs	Δt	$v_{\mathrm{TAS}} = 0\,\mathrm{m/s}$

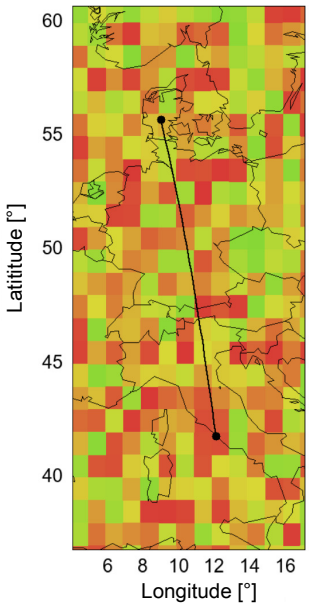

Figure 2: In the traffic flow analysis, the number of potential conflicts and the controller task load is calculated in a graticule grid (colored airspaces).

trajectories are clustered with regard to their mean track between the entry and exit points of the airspace. The clusters are sorted according to the number of associated trajectories. The cluster with the most associated trajectories is considered the main traffic flow, so it is preferred in the next optimization run. Among various methods for cluster analysis [38–41], a Density-Based Spatial Clustering of Applications with Noise (DBSCAN) [42] has been chosen, constructing clusters according to the idea that items are grouped in an n-dimensional space that is close to one another. The advantage of this algorithm is that the number of clusters is not an input variable but estimated by DBSCAN. Areas with lower densities of objects separate the clusters from one another. For this reason, parameters are set to specify the distance measure and the bare minimum of items needed to create a cluster. If the minimum number of items is attained or exceeded within the specified distance, the environment is considered dense.

Beyond the three most common density-based techniques (i.e., the Ordering Points To Identify the Clustering Structure (OPTICS) [43], the Maximum Margin Clustering [44], and the Density-Based Spatial Clustering of Applications with Noise DBSCAN, DBSCAN is the most common one when considering noise and it is used in this study with the parameters ε [a.u.] and Min_c [a.u.]. In this study, we calculate the minimum number of objects Min_c, which must be located within a fixed radius ε of a data point called the core point, in order for there to be a dense environment.

$$Min_c = \max\left[3, \frac{N_{\mathrm{aircraft,FL}}}{5}\right] \tag{1}$$

is a function of $N_{\mathrm{aircraft,FL}}$ the number of aircraft per flight level and airspace. Thus, a minimum of three aircraft to create a cluster is guaranteed. At flight levels and in airspaces with lots of aircraft, Min_c is restricted to avoid creating too many clusters.

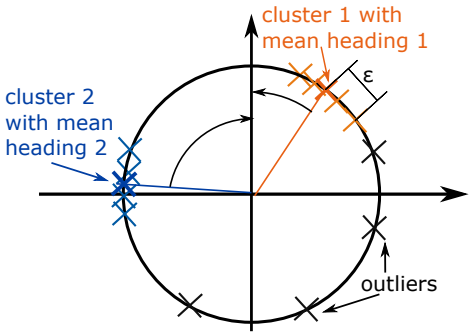

Figure 3: 2D DBSCAN cluster analysis of aircraft tracks within airspace. By placing each point on a unit circle according to their track, tracks with 359° are close to tracks with 1°. ε defines the maximum difference between the core points (thick crosses) and data points belonging to the cluster.

After clustering, the identified main track flow of the data points that make up each overloaded airspace and the number of potential conflicts inside each overloaded airspace are stored. For overloaded airspaces, we define a new cost layer with benefits for those aircraft with tracks close to the main traffic flow.

C. Definition of new cost layer with reduced costs along main traffic flows

The costs for flying along two nodes 1 and 2 within overloaded airspace are defined as

$$C_{\mathrm{s}} = \frac{a\, d\, N_{\mathrm{conflict,FL}} \sin\frac{\alpha}{2}}{N_{\mathrm{aircraft,FL}}}, \tag{2}$$

where a [m/€] is a proportional factor for adjustment and is adjusted iteratively for receiving minimum total cost

solutions in the purple loop. In this study, $a = 1\,\mathrm{m}/€$ d [m] denotes the distance between two nodes, $N_{\mathrm{conflict,FL}}$ is the number of conflicts in the airspace at a specific flight level, α the angle between the track between two nodes and the main track of the nearest cluster. Again, $N_{\mathrm{aircraft,FL}}$ denotes the number of aircraft at a specific flight level in the airspace (see Figure 4). The costs for flying through the overloaded airspace increase with increasing distance d and an increasing number of conflicts in the airspace N_{conflict} (Equation 2). On the other hand, the costs decrease with an increasing number of aircraft in the airspace at the concerned flight level $N_{\mathrm{aircraft,FL}}$, because aircraft should be attracted to join the main air traffic flow. The term $\sin\frac{\alpha}{2}$ guarantees that maximum costs occur for flows in opposite directions (i.e. $\alpha = \pi$) and minimum costs occur for flows with equal tracks ($\alpha = 0$). Note, N_{conflict} can be replaced or extended by the controller's task load.

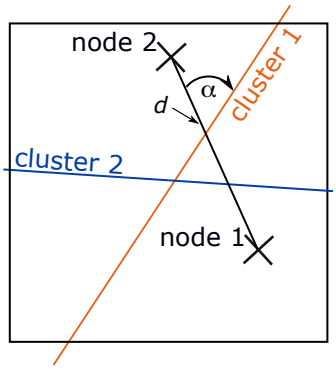

Figure 4: Definition of angle α between two nodes and the main track of the nearest cluster. Distance d defines the distance between two neighbored nodes in the airspace.

IV. Results

A. First Version

The method described in Section III is implemented in an air traffic scenario consisting of 72 flights crossing Central Europe, departing at the same time and inducing a large number of potential conflicts over Central Europe (see Figure 5). As described in Section II in the first control loop (blue in Figure 1), the weather-optimal altitude (with respect to minimum fuel) is estimated within eight iterations (between $\mathrm{FL_{min}} = 250$ and $\mathrm{FL_{max}} = 400$) neglecting continuous cruise climb (see Figure 6).

Since "minimum fuel" is an analytically solvable optimization target function for SOPHIA, true airspeed, climb- and descent rates are already optimized in the blue loop and the gray loop can be avoided in the first version. The ATFM assessment yielded in $N_{\mathrm{airspace,overl.}} = 9$ overloaded sectors and $N_{\mathrm{conflict}} = 336$ potential conflicts, corresponding with an average of 4.8 conflicts per flight. The average fuel burn per flight was $m_{\mathrm{fuel}} = 4135\,\mathrm{kg}$ with an average flight time of $t_{flight} = 7318\,\mathrm{s}$.

B. Iterative ATFM-optimization

In total, we identified 24 airspaces with more than ten potential conflicts. For the identified overloaded airspaces,

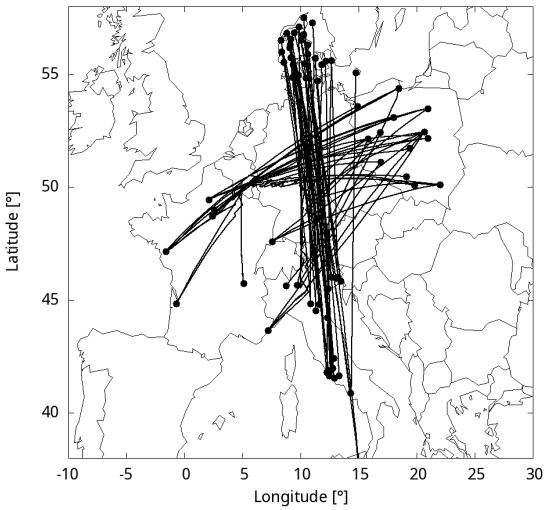

Figure 5: Initial situation: 72 flights crossing Central Europe departing at the same time inducing a large number of conflicts. During the initial simulation run (i.e. the first version), no airspace costs are applied.

airspace costs are calculated according to Equation 2. After the third iteration (v3), $N_{\mathrm{airspace,overl.}}$ decreased to one-third (see Table II), whereas the total number of conflicts N_{conflict} is minimized after four iterations. Note, a minimum number of potential conflicts is the termination criterion.

TABLE II. Iterative reduction of overloaded airspaces and potential conflicts due to track-specific airspace costs in the path-finding algorithm. M_{fuel} and t_{flight} denote average values per flight.

Iteration	$N_{\mathrm{airspace,overl.}}$	N_{conflict}	M_{fuel} [kg]	t_{flight} [s]
v0	9	336	4135.12	7318
v1	8	299	4136.33	7337
v2	6	272	4143.95	7345
v3	5	265	4140.84	7341
v4	3	253	4141.46	7339
v5	6	280	4138.02	7329

For every single trajectory, only FL 390 and FL 400 were identified as optimal. Considering the iteratively adjusted airspace costs (Equation 2), the variance in optimum cruising altitudes increased and lower altitudes are considered (see Figure 6), whereby average fuel burn M_{fuel} [kg] and flight time t_{flight} [s] did not increase significantly (see Table II).

Figure 6 follows that altitude changes are an effective strategy for reducing the number of potential conflicts, induced by flight level-specific airspace costs.

After two iterations (i.e. three versions), the total number of conflicts could be reduced from 330 to 227 by 32 % with an increase in fuel burn of 5 kg or 1,2 % (which is beyond the accuracy of SOPHIA's fuel precision) and an increase in flight time of 20 s or 2,7 % (which is not worth mentioning).

Unfortunately, not all airspaces benefit from this procedure. Even after lots of iterations, the remaining overloaded

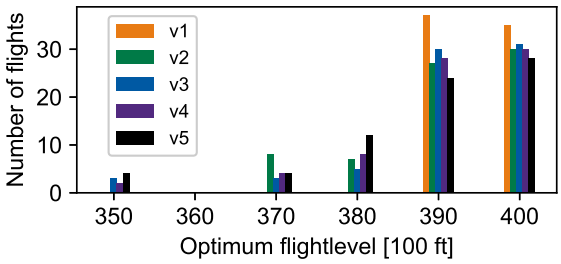

Figure 6: Shift in optimal cruise altitudes due to FL-specific airspace costs.

airspaces could not be disburdened. Those airspaces hold a large number of potential conflicts. In two airspaces, the number of potential conflicts increased with an increasing number of iterations. Handling those airspaces poses a challenge to this method. A solution could be to artificially increase the airspace costs in airspaces with an extremely high number of conflicts or with an increasing number of conflicts after two subsequent iterations. One of those airspaces counted for a maximum of 28 potential conflicts per airspace has been identified. Although this is an exception, Figure 7 shows a satisfactory frequency distribution of conflicts per airspace and a decreasing number of conflicts after each iteration.

C. Stochastic approach

Since the reduction of the number of both potential conflicts and overloaded airspaces may be more efficiently reached with flight level changes instead of track changes after introducing airspace costs, the optimum altitude of each aircraft might still be the same. This means several aircraft will divert in the same direction and the overloaded airspace may only be shifted vertically. In this case, $N_{\mathrm{conflict,FL}}$ and the number of overloaded airspaces might not be reduced. For this reason, airspace costs can also be assigned to only a part of the aircraft in conflict. For example, Table III shows the solution in case only $50\,\%$ of the aircraft (randomly chosen) are burdened with airspace costs. Therewith, the total number of overloaded airspaces could be reduced to 3 (instead of 4) without serious changes in fuel burn or flight time. Although the results are promising, the non-guaranteed equal treatment of all flights possibly complicates the acceptance of the method for operational ATFM.

TABLE III. Improved reduction of overloaded airspaces and potential conflicts by assigning airspace costs only to $50\,\%$ of the aircraft in conflict (per overloaded airspace and flight level). M_{fuel} and t_{flight} denote average values per flight.

Iteration	$N_{\mathrm{airspace,overl.}}$	N_{conflict}	M_{fuel} [kg]	t_{flight} [s]
v0	9	336	4135.12	7318
v1	7	302	4136.07	7333
v2	3	247	4138.43	7331
v3	2	199	4137.57	7333
v4	4	198	4137.51	7332

V. Conclusion

In this paper, we have shown a new iterative approach to considering the interactions of different trajectories in a single-flight-based simulation environment. By identifying overloaded airspaces in a flight-level-specific manner and extracting major traffic flows in these airspaces, airspace cost layers for the path search algorithm with track-specific costs were created for all affected flight levels. With this additional cost layer, the single flight optimization was performed again and then the number of congested airspaces was counted repeatedly.

The procedure has been implemented and tested on a set of 72 aircraft trajectories, all crossing central Europe at the same time. In total 90 airspaces were analyzed, overloaded airspaces were identified, main tracks within the overloaded airspaces were determined and track-and altitude-specific airspace costs for those airspaces were provided to the path-finding algorithm. Within a surprisingly small number of iterations, the number of overloaded airspaces and the number of conflicts could be minimized. Aircraft were successfully encouraged to follow main tracks within the airspace, or laterally or vertically avoid overloaded airspaces.

Despite all this, this is the first attempt to solve ATFM concerns with TOMATO without giving up flexibility and precision in the optimization of the single trajectory. Some weaknesses of the methods have been identified and will be improved shortly.

Firstly, the task load of the controller is integrated into the calculation of the airspace costs. For this purpose, either Equation 2 could be extended or a two-step or conditional calculation rule for the airspace costs could be developed. The task load is flight time dependent. However, the path-finding algorithm usually does not know how long the aircraft will be in the airspace. This has so far been solved for other cost layers by iteratively determining mean values. Difficulties are expected here for the airspace costs, which have not been dealt with so far.

Second, we are dissatisfied with the definition of the self-defined minimum number of conflicts of congested airspaces and hope for more precise values through expert interviews. Another possibility would be to derive the volatility and appropriate values for the number of main tracks per airspace from real flight scenarios (e.g. from an ADS-B data analysis). The only free variable that remains would be the minimum number of potential conflicts, which we assume the pilot does not want to solve tactically.

We are also looking for a fast optimization method for the optimal cruising altitude including flight level changes and continuous cruise climb segments. Our previously purely iterative method is simply too slow for ATFM concerns.

References

[1] A. Odoni, L. Bianco, and G. Szego, *The Flow Management Problem in Air Traffic Control*. Springer, Berlin, 1987.

[2] International Civil Aviation Organization, "Procedures of air navigation services, air traffic management," Doc. 4444 PANS-ATM, Montreal, Canada, 2016.

[3] S. Förster, J. Rosenow, M. Lindner, and H. Fricke, "A toolchain for optimizing trajectories under real weather conditions and

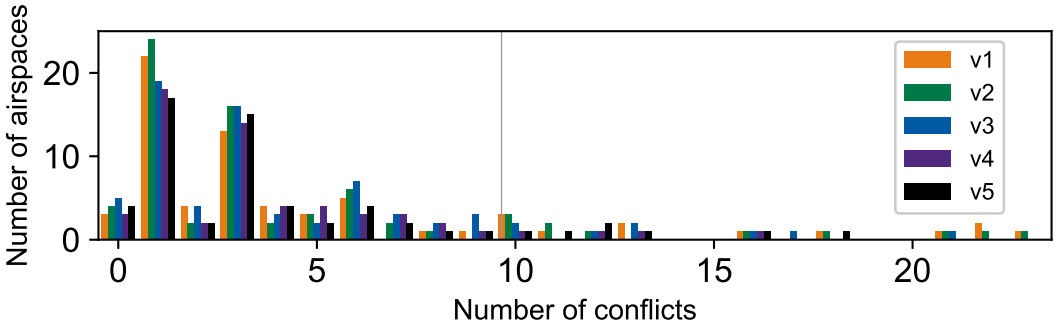

Figure 7: Iterative reduction of conflicts per airspace. Overloaded airspaces have $N_{\max} \leq 10$ conflicts.

realistic flight performance," in *Greener Aviation, Brussels*, 2016.

[4] A. Marzuoli, M. Gariel, A. Vela, and E. Feron, "Air traffic optimization on data-driven network flow model," in *2011 IEEE/AIAA 30th Digital Avionics Systems Conference*, 2011, pp. 1–21.

[5] E. Salaun, M. Gariel, A. E. Vela, and E. Feron, "Aircraft proximity maps based on data-driven flow modeling," *Journal of Guidance, Control, and Dynamics*, vol. 35, no. 2, pp. 563–577, 2012. [Online]. Available: https://doi.org/10.2514/1.53859

[6] M. Gariel, A. N. Srivastava, and E. Feron, "Trajectory clustering and an application to airspace monitoring," *IEEE Transactions on Intelligent Transportation Systems*, vol. 12, no. 4, pp. 1511–1524, 2011.

[7] G. Sabhnani, A. Yousefi, I. Kostitsyna, J. Mitchell, V. Polishchuk, and D. Kierstead, *Algorithmic Traffic Abstraction and its Application to NextGen Generic Airspace*. [Online]. Available: https://arc.aiaa.org/doi/abs/10.2514/6.2010-9335

[8] D. Bertsimas, G. Lulli, and A. Odoni, "The air traffic flow management problem: An integer optimization approach," 05 2008, pp. 34–46.

[9] H. Balakrishnan and B. G. Chandran, "Optimal large-scale air traffic flow management," 2014.

[10] D. Toratani, "Application of merging optimization to an arrival manager algorithm considering trajectory-based operations," *Transportation Research Part C: Emerging Technologies*, vol. 109, pp. 40–59, 12 2019.

[11] M. Soler, B. Zou, and M. Hansen, "Flight trajectory design in the presence of contrails: Application of a multiphase mixed-integer optimal control approach," *Transportation Research Part C: Emerging Technologies*, vol. 48, pp. 172–194, 2014.

[12] J. Rosenow, "Multi-criteria aircraft trajectory optimization, the environmental footprint of aviation," Ph.D. dissertation, Technische Universität Dresden, 2022.

[13] P. E. Hart, N. Nilsson, and B. Raphael, "A formal basis for the heuristic determination of minimum cost paths," *IEEE Transactions on Systems Science and Cybernetics*, vol. 4, no. 2, pp. 100–7, 1968.

[14] J. Rosenow, G. Chen, H. Fricke, and Y. Wang, "Factors impacting chinese and european vertical fight efficiency," *Aerospace*, vol. 9, no. 2, 2022. [Online]. Available: https://www.mdpi.com/2226-4310/9/2/76

[15] J. Rosenow, S. Förster, and H. Fricke, "Continuous climb operations with minimum fuel burn," in *Sixth SESAR Innovation days*, 2016.

[16] J. Rosenow, D. Strunck, and H. Fricke, "Trajectory optimization in daily operations," in *International Conference on Research in Air Transportation (ICRAT)*, 2018.

[17] M. Lindner, J. Rosenow, T. Zeh, and H. Fricke, "In-Flight Aircraft Trajectory Optimization within Corridors Defined by Ensemble Weather Forecasts," *Aerospace*, vol. 7, no. 10, p. 144, Oct. 2020.

[18] M. Lindner, T. Zeh, H. Braßel, J. Rosenow, and H. Fricke, "Traffic flow funnels based on aircraft performance for optimized departure procedures," *Future Transportation*, vol. 2, no. 3, pp. 711–733, 2022. [Online]. Available: https://www.mdpi.com/2673-7590/2/3/40

[19] J. Rosenow and H. Fricke, "When do contrails cool the atmosphere?" in *SESAR Innovation Days (SID 2022)*, 2022, Budapest, Hungary. [Online]. Available: https://www.researchgate.net/publication/366905171_When_do_contrails_cool_the_atmosphere

[20] J. Rosenow, S. Förster, M. Lindner, and H. Fricke, "Multicriteria-optimized trajectories impacting today's air traffic density, efficiency, and environmental compatibility," *Journal of Air Transportation*, 2018.

[21] European Civil Aviation Conference, "Report on standard method of computing noise contours around civilairports – volume 1: Applications guide," *Neuilly-sur-Seine*, vol. ECAC 29, 2016.

[22] ——, "Report on standard method of computing noise contours around civilairports – volume 2: Technical guide," *Neuilly-sur-Seine*, vol. ECAC 29, 2016.

[23] T. Zeh, M. Lindner, J. Rosenow, and H. Fricke, "Optimization of departure routes beyond aircraft noise abatement," in *International Conference on Research in Air Transportation (ICRAT 2022)*, 2022, Tampa, Florida.

[24] National Oceanic and Atmospheric Administration. (2016) Global data assimilation system (gdas). [Online]. Available: ncei.orders@noaa.gov

[25] M. Lindner, J. Rosenow, and H. Fricke, "Aircraft trajectory optimization with dynamic input variables," *CEAS Aeronautical Journal*, vol. 11, no. 2, pp. 321–331, 2020. [Online]. Available: https://doi.org/10.1007/s13272-019-00430-0

[26] R. P. Brent, "An algorithm with guaranteed convergence for finding a zero of a function," *The computer journal*, vol. 14, no. 4, pp. 422–425, 1971.

[27] J. Rosenow, S. Förster, M. Lindner, and H. Fricke, "Multi-objective trajectory optimization," *International Transportation*, vol. Special Edition 1, 2016.

[28] J. Sun, J. M. Hoekstra, and J. Ellerbroek, "Openap: An open-source aircraft performance model for air transportation studies and simulations," *Aerospace*, vol. 7, no. 8, 2020. [Online]. Available: https://www.mdpi.com/2226-4310/7/8/104

[29] T. Zeh, J. Rosenow, R. Alligier, and H. Fricke, "Prediction of the Propagation of Trajectory Uncertainty for Climbing Aircraft," in *39th AIAA/IEEE Digital Avionics Systems Conference*, San Antonio, TX, 2020.

[30] J. Rosenow, T. Sachwitz, S. Kamo, G. Chen, and H. Fricke, "Aircraft-type-specific impact of speed brakes on lift and drag," *Aerospace*, vol. 9, no. 5, 2022. [Online]. Available:

https://www.mdpi.com/2226-4310/9/5/263
[31] A. Cook and G. Tanner, “European airline delay cost reference values,” University of Westminster, v4.1, 2015.
[32] T. Mofokeng, P. Mativenga, and A. Marnewick, “Analysis of aircraft maintenance processes and cost,” *Procedia CIRP*, vol. 90, pp. 467–472, 01 2020.
[33] International Air Transport Association. (2023) Jet fuel price monitor. [Online]. Available: https://www.iata.org/en/publications/economics/fuel-monitor/
[34] J. Rosenow, P. Michling, M. Schultz, and J. Schönberger, “Evaluation of strategies to reduce the cost impacts of flight delays on total network costs,” *Aerospace*, vol. 7, no. 11, 2020. [Online]. Available: https://www.mdpi.com/2226-4310/7/11/165
[35] D. S. Lee, G. Pitari, V. Grewe, K. Gierens, J. E. Penner, A. Petzold, M. J. Prather, U. Schumann, A. Bais, T. Berntsen, D. Iachetti, L. L. Lim, and R. Sausen, “Transport impacts on atmosphere and climate: Aviation,” *Atmospheric Environment*, vol. 44, pp. 4678–4734, 2010.
[36] J. Rosenow and H. Fricke, “Individual condensation trails in aircraft trajectory optimization,” *Sustainability*, vol. 11, no. 21, 2019. [Online]. Available: https://www.mdpi.com/2071-1050/11/21/6082
[37] European Environment Agency. (2023) Eu emissions trading system (ets) data viewer. [Online]. Available: https://www.eea.europa.eu/data-and-maps/dashboards/emissions-trading-viewer-1
[38] H. Driver and A. Kroeber, “Quantitative expression of cultural relationships,” *University of California Publications in American Archaeology and Ethnology*, vol. Quantitative Expression of Cultural Relationships, pp. 211–256, 09 1932.
[39] J. Zubin, “A technique for measuring like-mindedness,” *The Journal of Abnormal and Social Psychology*, vol. 33, pp. 508–516, 09 1938.
[40] R. Tryon, *Cluster analysis; correlation profile and orthometric (factor) analysis for the isolation of unities in mind and personality*. Ann Arbor, Mich., Edwards Brother, Inc., lithoprinters and Publishers, 09 1939.
[41] R. Cattell, “The description of personality: basic traits resolved into clusters. the journal of abnormal and social psychology,” *The Journal of Abnormal and Social Psychology*, vol. 38, p. 476–506, 1943.
[42] M. Ester, H. Kriegel, J. Sander, and X. Xu, “A density-based algorithm for discovering clusters in large spatial databases with noise,” in *Proceedings of the Second International Conference on Knowledge Discovery and Data Mining (KDD-96). AAAI Press.*, 1996, pp. 226–231.
[43] M. Ankerst, M. Breunig, H. Kriegel, and J. Sander, “Optics: Ordering points to identify the clustering structure,” in *ACM SIGMOD international conference on Management of data. ACM Press.*, 1999, p. 49–60.
[44] L. Xu, J. Neufeld, B. Larson, and D. Schuurmans, “Maximum margin clustering,” in *Advances in Neural Information Processing Systems 17 [Neural Information Processing Systems, NIPS 2004, December 13-18, Vancouver, British Columbia, Canada*, 2004.